

Phase Behavior of Partially Miscible Blends of Linear and Branched Polyethylenes

C. H. Stephens, A. Hiltner,* and E. Baer

Department of Macromolecular Science and Engineering and Center for Applied Polymer Research, Case Western Reserve University, Cleveland, Ohio 44106-7202

Received October 25, 2002; Revised Manuscript Received January 20, 2003

ABSTRACT: Miscibility of Ziegler–Natta catalyzed high density polyethylene (HDPE) of broad molecular weight distribution with a homogeneous ethylene–octene copolymer (EO) of relatively narrow molecular weight distribution was studied as a function of constituent molecular weight and comonomer content. Blends were rapidly quenched from the melt to retain the phase morphology, and the phase volume fractions were obtained from AFM images. A homogeneous ethylene–octene copolymer with 5.3 mol % comonomer was completely miscible with high-density polyethylene, whereas copolymers with 8.5 and 12.3 mol % comonomer demonstrated a blend composition window for partial miscibility as indicated by phase volume fractions different from blend volume fractions. The temperature dependence of blend morphology confirmed the UCST behavior of EO/HDPE blends. The phase composition and the χ interaction parameter were extracted by using an approach that considered the molecular weight distribution. The solubility parameters obtained from the analysis agreed with literature values. The study demonstrated the general consequences for phase behavior of the low and high molecular weight tails on the broad distribution of HDPE. Even in EO copolymers with relatively narrow molecular weight distribution, preferential solubility of low molecular weight fractions in the HDPE-rich phase was clearly evident.

Introduction

Conventional copolymerization of ethylene and an α -olefin with a Ziegler–Natta catalyst results in a linear low-density polyethylene (ZN-LLDPE) with broad molecular weight distribution and heterogeneous short chain branch distribution. Heterogeneity in ZN-LLDPE takes the form of concentration of branches in lower molecular weight molecules. Characterization of a ZN-LLDPE fractionated by short chain branch content using preparative TREF demonstrated the broad range in composition and physical properties of the constituent molecules of ZN-LLDPE.¹ Binary blends of the lowest and the highest branch content fractions appeared to be immiscible.² Phase separation of highly branched molecules in unfractionated ZN-LLDPE was hypothesized on the basis of scanning electron microscopy.³ Recognizing that crystallization can produce phase separation in mixtures even if the melt is homogeneous, the melt structure of ZN-LLDPE has been probed directly. Small-angle neutron scattering (SANS) cross sections supported the hypothesis that a highly branched fraction of ZN-LLDPE can phase separate to form a disperse phase in the melt.⁴

The conventional methods for determining polymer/polymer miscibility are not amenable to blends of ethylene copolymers due to the chemical similarity of the constituents. Direct observation of phase behavior in the melt is possible with SANS provided one constituent is deuterated to achieve contrast. Experiments on blends of linear polyethylene with low-density polyethylene (LDPE) or model copolymers confirm that the mixtures are homogeneous for all compositions when the branch content is less than four branches per 100 backbone carbon atoms for molecular weight $M_w \approx 10^5$; however, the blends phase separate if the branch

content is higher than eight branches per 100 backbone carbon atoms.^{5,6} Miscibility of copolymers with branch content intermediate between 4 and 8 per 100 backbone carbon atoms was not discussed. Molecular dynamics simulation reproduced the limit of miscibility as four branches per 100 backbone carbon atoms.⁷

The SANS requirement for deuteration of one constituent introduces complications by way of an isotopic contribution to the thermodynamic interactions.^{8,9} In some cases, the effect can lead to isotope-driven phase separation.¹⁰ There are also concerns that the SANS method cannot differentiate a homogeneous melt from a biphasic melt with very large domain size.^{6,11} Nevertheless, the SANS approach has yielded important insights into the thermodynamics of ethylene copolymer blends by focusing on homogeneous blends of model polymers that are monodisperse in molecular weight and homogeneous in composition. Studies confirm the Flory–Huggins expression for the free energy of mixing to be a reliable framework for quantifying interactions in saturated hydrocarbon polymer blends and demonstrate that the interaction strengths for most saturated hydrocarbon blends obey the solubility parameter formalism.¹² Additional studies extend the validity of the solubility parameter formalism to blends of deuterated model polymers with polydisperse homogeneous metallocene copolymers.¹³

Motivated by the impracticality of producing labeled materials for SANS experiments, many studies of real polyolefin blends rely on rapid quenching to preserve the phase condition in the melt. Extremely rapid quenching is required if morphological artifacts brought about by crystallization during cooling are to be avoided.¹⁴ Despite concerns regarding crystallization-induced phase separation, domain morphologies of rapidly quenched blends observed by transmission electron microscopy (TEM) and atomic force microscopy (AFM) are coarse

* Corresponding author.

enough to conclude that crystallization does not account for phase separation.^{15–17} Rather, it appears that rapid crystallization reliably freezes the phase condition as it exists in the melt. Characterization of blends that combined a homogeneous ethylene–octene copolymer containing 14.6 mol % octene (melt index 0.5) with copolymers containing 8.5, 5.3, and 3.3 mol % octene (melt index 1.0) determined that only the copolymer with 8.5 mol % octene was miscible.¹⁸ Thus, the difference in comonomer content required for miscibility lay between 6 and 9 mol % for octene copolymers of this molecular weight. Other efforts to infer phase behavior of polyolefin blends from DSC thermograms or from lamellar textures in TEM and AFM images have not necessarily been conclusive, and in some cases contradictory results were reported.¹⁹

Two recent developments greatly facilitate the study of real polyolefin blends. Advances in catalyst technology allow for synthesis of copolymers of ethylene and an α -olefin with homogeneous comonomer distribution and narrow molecular weight distribution. These copolymers are excellent models for studying miscibility of ethylene copolymers. Furthermore, with AFM, it is possible to directly image the phase morphology of ethylene copolymer blends rapidly quenched from the melt. Tapping mode AFM is sufficiently sensitive to small modulus differences that it can image phase morphology in blends of chemically similar species.

The opportunity afforded by these advances was demonstrated in studies of amorphous ethylene–styrene copolymer blends. Largely based on AFM images of the domain morphology, these studies characterized the phase diagram, established the existence of an upper critical solution temperature, and identified the transition from miscible to immiscible copolymer blends at 9 wt % difference in comonomer.²⁰ Further probes of a very small region in composition where partial miscibility was evident, 9–10 wt % difference in styrene content, revealed the dependence of phase composition on initial blend composition and emphasized the role of molecular weight distribution.²¹ The consequences of polydispersity were considered according to a theoretical treatment that incorporated the molecular weight distribution. The results demonstrated the validity of the copolymer equation for describing the interaction parameter χ of these copolymers and enabled the molecular weight distribution of the constituents in each phase to be determined.

The present study was undertaken to determine whether the approach used with amorphous ethylene–styrene copolymer blends could be extended to blends of crystallizable ethylene polymers. Three high density polyethylenes (HDPEs) were each blended with four homogeneous metallocene ethylene–octene copolymers (EOs). The effect of short chain branch content was examined with EOs of approximately the same molecular weight that differed in comonomer content. The role of molecular weight was examined with HDPEs that differed in molecular weight and polydispersity and also with EOs of the same comonomer content that differed in molecular weight.

Materials and Methods

The homogeneous ethylene–octene copolymers described in Table 1 were provided as pellets by The Dow Chemical Co.²² The copolymers are identified by the prefix EO followed by the octene content as mole percent. Two copolymers with 12.3 mol % octene that differed in molecular weight are differenti-

Table 1. Characteristics of Polyethylene Resins

polymer	octene content (mol %)	octene content (wt %)	M_w (g/mol)	M_w/M_n	density (g/cm ³)	cryst ^a (wt %)
EO5.3	5.3	18.2	89 400	2.3	0.9014	33
EO8.5	8.5	27.1	98 200	2.2	0.8882	25
EO12.3LMW	12.3	35.9	52 300	2.0	0.8711	14
EO12.3HMW	12.3	35.9	147 100	2.1	0.8751	14
HDPE62	0.0	0.0	61 800	4.8	0.9561	70
HDPE137	0.0	0.0	137 300	7.3	0.9555	68
HDPE292	0.0	0.0	292 300	10.9	0.9560	70

^a Key: cryst = crystallinity.

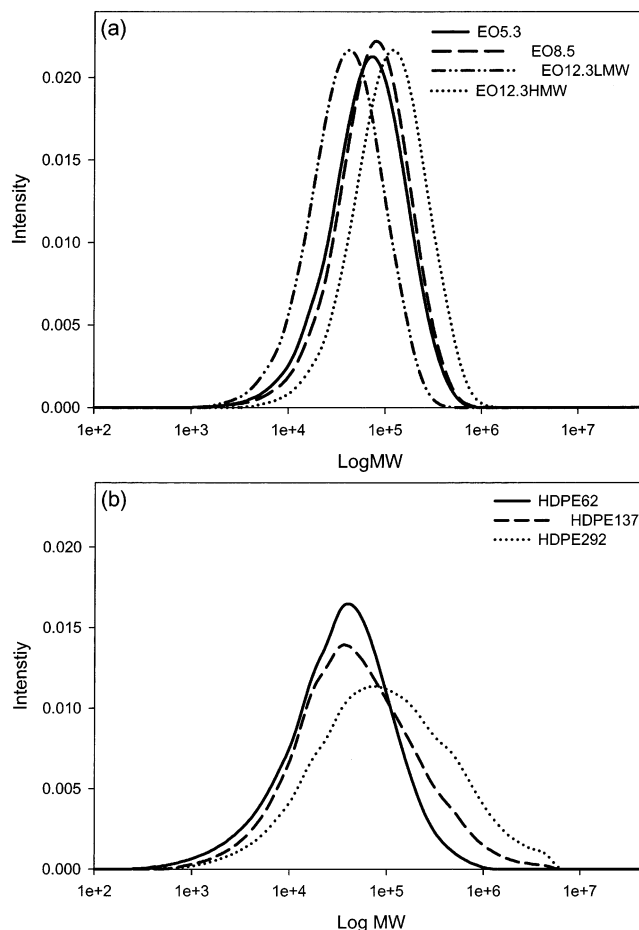


Figure 1. Molecular weight distributions as weight fractions: (a) ethylene–octene copolymers; (b) high-density polyethylenes. Peak areas are normalized to unity.

ated by the suffixes LMW and HMW. The high-density polyethylene resins were provided as pellets or powder by BP Chemicals. They are designated by the prefix HDPE followed by the molecular weight as kg mol⁻¹. Molecular weight distributions were determined by GPC operating at 140 °C with trichlorobenzene as the solvent. Polystyrene standards were used for calibration. Data were obtained in digital format in 190 equal log M increments. Molecular weight distributions of the EO copolymers are shown in Figure 1a, those of the HDPE resins are shown in Figure 1b.

Density of slowly cooled compression molded films was determined using a density gradient column. Water and 2-propanol were mixed according to ASTM-1505-85. The error in the density determination was no greater than 0.0003 g cm⁻³. Crystallinity of compression molded films was determined using a Perkin-Elmer model 7 DSC. Thermograms were obtained with a heating rate of 10 °C min⁻¹. Crystallinity was calculated from a heat of fusion of 290 J g⁻¹ for the polyethylene crystal.²³

Blends were prepared by weighing the appropriate amount of each constituent (vol/vol) and dissolving the resulting dry mixture in sufficient xylene to give a 5 wt % solution. The mixture was stirred at ambient temperature overnight and heated with stirring at 130 °C for 1 h. Blends were precipitated by pouring the solution into an excess of stirred methanol that was chilled in a dry ice/methanol bath. The precipitated blend was filtered and dried in a vacuum for 48 h at ambient temperature.

Blends were prepared for AFM imaging by melting approximately 40 mg in an uncovered pan under nitrogen in a Rheometrics DSC. Specimen size was minimized in order to achieve as rapid a cooling rate as possible during quenching. Specimens melted at 150, 165, 180, and 210 °C were held at temperature for 1 h. Those melted at 240 and 270 °C were held at temperature for 30 min. Seemingly long melt times were used to allow for phase coarsening. The possibility of polymer degradation was tested at 270 °C by melting the partially miscible EO12.3LMW/HDPE62 70/30 blend for 15 min before quenching. The phase volume fractions (0.88/0.12) were the same within experimental error as those for the blend melted for 30 min (0.89/0.11). Concerns for polymer degradation prevented investigation of higher melt temperatures. To freeze in the phase morphology at the melt temperature, specimens were quenched from the melt by rapidly removing the pan from the DSC and plunging it into an acetone/dry ice mixture.¹⁷

Specimens were microtomed at -75 °C to expose the bulk morphology and etched for 30 min using a 2:1:0.07 sulfuric acid-*o*-phosphoric acid-potassium permanganate solution²⁴ to remove surface marks caused by microtoming. Tapping mode AFM was performed using a Digital Laboratories Nanoscope IIIa with a Multimode head and J-scanner. All measurements were made at ambient temperature, and intermediate to hard tapping was employed to reveal good contrast in both height and phase images.

Although the modulus difference between phases was large enough to reveal the domain morphology in AFM phase images of immiscible or partially miscible blends, AFM height images generally provided better resolution, particularly if the harder HDPE-rich phase was the dispersed phase. Therefore, primarily blend compositions with EO as the major constituent were analyzed. Generally, 10 μ m height images provided both good resolution of the phase morphology and a statistical cross-section. The phase boundaries were traced by hand and converted to electronic form by scanning with Adobe Photoshop software. Image analysis with Image-Pro Plus software from Media Cybernetics gave the amount of each phase. In all cases, the image analyzed was at least 15 times larger than the phase dimension. Results from four unique images were averaged to obtain phase volume fractions.

Results and Discussion

Phase Behavior. A homogeneous, single-phase morphology in AFM images of EO5.3 blended with all three HDPEs revealed that these blends were miscible in all compositions and at all temperatures studied. At the other extreme, EO12.3LMW and EO12.3HMW blended with either HDPE137 or HDPE292 formed phase-separated morphologies in which the phase volume fractions were the same as the blend composition. These blends were essentially immiscible. This result conformed with a previous finding that the difference in comonomer content required for miscibility of two homogeneous ethylene-octene copolymers is between 6 and 9 mol %.¹⁸

The present study probed the narrow range of compositional difference in which partial miscibility was observed. Representative AFM height and phase images of the 60/40 (v/v) EO8.5/HDPE137 blend quenched from three melt temperatures are compared in Figure 2. The modulus difference between phases was large enough

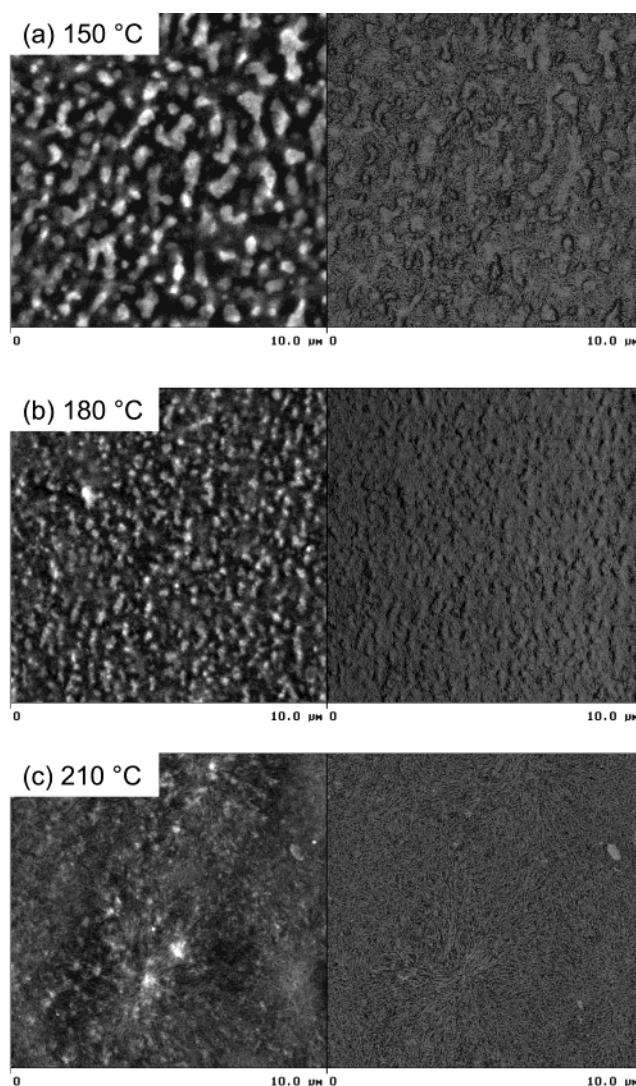


Figure 2. AFM height (left side) and phase (right side) images of 60/40 (v/v) EO8.5/HDPE137 blends: (a) quenched from 150 °C; (b) quenched from 180 °C; (c) quenched from 210 °C.

to reveal phase separation, however height images provided better contrast between phases. Therefore, blends were categorized as miscible or two-phase based on phase images, and height images were analyzed for phase volume fractions. The specimens quenched from 150 and 180 °C in Figure 2a,b showed two phases, indicating that EO8.5/HDPE137 60/40 was not completely miscible at these temperatures. However, a specimen quenched from 210 °C exhibited a homogeneous, single-phase morphology in the phase image, Figure 2c. The texture in the corresponding height image was caused by surface roughness. It was apparent that EO8.5/HDPE137 blends exhibited an upper critical solution temperature (UCST).

Blends of EO8.5 with all the HDPEs, and blends of EO12.3LMW and EO12.3HMW with HDPE62 exhibited partial miscibility as indicated by phase volume fractions that were different from the blend composition, Table 2. As melt temperature increased, the volume fraction of the major phase increased until in some cases a single phase was achieved. This confirmed that all of the blends exhibited UCST behavior.

The UCST could not be determined directly by AFM imaging because of insufficient contrast between the

Table 2. Relative Phase Compositions from AFM Image Analysis

blend constituents	T (°C)	EO/HDPE 70/30			60/40			40/60			30/70		
		EO-rich (vol. %)	HDPE-rich (vol. %)	error (±)	EO-rich (vol. %)	HDPE-rich (vol. %)	error (±)	EO-rich (vol. %)	HDPE-rich (vol. %)	error (±)	EO-rich (vol. %)	HDPE-rich (vol. %)	error (±)
EO8.5/HDPE62	150	0.88	0.12	0.01	0.72	0.28	0.01						
	165	miscible			0.93	0.07	0.01						
	180				miscible								
EO8.5/HDPE137	150	0.81	0.19	0.04	0.66	0.34	0.01	0.28	0.72	0.03	0.24	0.76	0.02
	165	0.83	0.17	0.00	0.74	0.26	0.01						
	180	0.86	0.14	0.02	0.81	0.19	0.02	miscible			miscible		
	210	miscible			miscible								
EO8.5/HDPE292	210	0.81	0.19	0.02	0.86	0.14	0.01						
	240	0.91	0.09	0.01	0.90	0.10	0.04						
	270	miscible			miscible								
EO12.3LMW/HDPE62	150										0.26	0.74	0.01
	180	0.81	0.19	0.02				0.32	0.68	0.12	0.16	0.84	0.01
	210	0.87	0.13	0.02	0.81	0.19	0.02	0.23	0.77	0.02	0.01	0.99	0.00
	240	0.98	0.02	0.00	0.94	0.06	0.01	miscible			miscible		
EO12.3HMW/HDPE62	180				0.71	0.29	0.04						
	210	0.80	0.20	0.01	0.72	0.28	0.01						
	240	0.84	0.16	0.02	0.77	0.23	0.01						
	270	0.89	0.11	0.04									

phases as they approached the same composition. However, from Table 2 it was possible to infer the effect of constituent molecular weight and EO comonomer content on the UCST. An increase in the temperature required to achieve miscibility of EO8.5/HDPE as the HDPE molecular weight increased from HDPE62 to HDPE137 to HDPE292 demonstrated that EO became less miscible as the HDPE molecular weight increased. Similarly, poorer miscibility of EO12.3HMW compared to EO12.3LMW in blends with HDPE62 was evident from the lower volume fraction of the major phase in the EO12.3HMW blend compared to the EO12.3LMW blend at each temperature. Complete miscibility of EO5.3/HDPE62 70/30 at all temperatures, miscibility of EO8.5/HDPE62 70/30 at 165 °C and only partial miscibility of EO12.3HMW/HDPE62 70/30 at 270 °C demonstrated that increasing EO comonomer content markedly reduced its miscibility with HDPE.

The Flory–Huggins description of a binary polymer mixture introduces the interaction parameter χ ,²⁵ which can be extracted from the formulation

$$\frac{\Delta G}{RT} = \frac{\phi_1}{N_1 v_1} \ln \phi_1 + \frac{\phi_2}{N_2 v_2} \ln \phi_2 + \frac{\chi}{v} \phi_1 \phi_2 \quad (1)$$

by application of the equilibrium condition for equality of constituent chemical potentials in both phases if the constituents are monodisperse. In eq 1, N_1 and N_2 are the degrees of polymerization of constituents 1 and 2, v_1 and v_2 are the average molar volumes of the constituent 1 and 2 monomers, v is the reference volume, and ϕ_1 and ϕ_2 are the volume fractions of constituents 1 and 2 in the blend. However, the strong molecular weight dependence of miscibility signifies that the molecular weight distribution of real polymers cannot be neglected even though the molecular weight distribution may be relatively narrow, as with homogeneous ethylene copolymers.²¹

A thermodynamic approach developed by Solc and co-workers incorporates the molecular weight distribution of the blend constituents.^{26–28} The validity of this approach to partially miscible ethylene copolymers with homogeneous composition and polydisperse molecular weight distribution was demonstrated previously.²¹ In the general case of two polydisperse constituents, the

free energy of mixing for a blend of composition ϕ_2 is given by

$$\frac{\Delta G}{RT} = \sum_i n_i \ln \phi_{1i} + \sum_j n_j \ln \phi_{2j} + \chi \phi_2 \sum_i n_i r_{1i} \quad (2)$$

where n is moles of chains and ϕ is volume fraction in the blend of the monodisperse fractions identified by subscripts i and j for constituents 1 and 2, respectively. The relative chain length r is defined as the number of basic units in a chain, and the volume fraction of such chains in the blend is $\phi_{1i} = n_i r_{1i} / r_{\text{total}}$ and $\phi_{2j} = n_j r_{2j} / r_{\text{total}}$ where $r_{\text{total}} = \sum n_i r_{1i} + \sum n_j r_{2j}$. Using the average monomer of constituent 1 as the basic unit, $r_{1i} = N_{1i}$ and $r_{2j} = N_{2j}(v_2/v_1)$, where N is the degree of polymerization and v_1 and v_2 are the average monomer volumes of constituents 1 and 2, respectively.

At equilibrium, the chemical potential of each constituent is the same in both phases. Thus, the calculation of equilibrium concentrations involves the solution for a system of equations. However, the number of equations can be reduced dramatically by introducing two separation factors, σ_1 and σ_2 , where the partitioning of each constituent between the two phases (indicated by ' and ') obeys the relation

$$\sigma_1 = r_{1i}^{-1} (\ln \phi'_{1i} - \ln \phi'_{1j}) \quad (3a)$$

and

$$\sigma_2 = r_{2j}^{-1} (\ln \phi'_{2j} - \ln \phi'_{2i}) \quad (3b)$$

for all i and j . Therefore, the system of equilibrium equations is reduced to two equations

$$\sigma_1 (\phi'_1 + \phi'_j) + \sigma_2 (\phi'_2 + \phi'_i) - 2 \left[\left(\frac{\phi'_1}{r'_{n1}} + \frac{\phi'_2}{r'_{n2}} \right) - \left(\frac{\phi'_1}{r'_{n1}} + \frac{\phi'_2}{r'_{n2}} \right) \right] = 0 \quad (4)$$

and

$$\sigma_2 - \sigma_1 = 2\chi(\phi'_1 - \phi'_j) \quad (5)$$

here r'_{n1} , r''_{n1} , r'_{n2} and r''_{n2} are the number-average chain lengths of each constituent in each phase

$$r'_{n1} = \phi'_1 \left(\sum_i \frac{\phi'_{1i}}{r_{1i}} \right)^{-1} \quad (6)$$

etc.

Additional mass balance equations are used to compute the phase compositions and χ . Volume additivity upon demixing gives

$$\phi'_{1i} + R_v \phi''_{1i} = (R_v + 1)\phi_{1i} = (R_v + 1)\phi_1 W_{1i} \quad (7a)$$

and

$$\phi'_{2j} + R_v \phi''_{2j} = (R_v + 1)\phi_{2j} = (R_v + 1)\phi_2 W_{2j} \quad (7b)$$

where $R_v = V'/V$ is the volume ratio of the two phases, ϕ_1 and ϕ_2 are the volume fractions of constituents 1 and 2 in the blend, and W_{1i} and W_{2j} are the weights of fractions i and j in constituents 1 and 2, respectively. Combining eq 7 with eq 3, the definition of the separation factor, gives

$$\phi'_1 = \sum_i \phi'_{1i} = (R_v + 1)\phi_1 \sum_i \frac{W_{1i}}{1 + R_v \exp(\sigma_1 r_{1i})} \quad (8a)$$

and

$$\phi'_2 = \sum_j \phi'_{2j} = (R_v + 1) \phi_2 \sum_j \frac{W_{2j}}{1 + R_v \exp(\sigma_2 r_{2j})} \quad (8b)$$

Finally, combining eq 8 with the mass balance expression $\phi_1 + \phi_2 = \phi'_1 + \phi'_2 = 1$ gives

$$\phi_1 \sum_i \frac{W_{1i}}{1 + R_v \exp(\sigma_1 r_{1i})} + \phi_2 \sum_j \frac{W_{2j}}{1 + R_v \exp(\sigma_2 r_{2j})} - \frac{1}{1 + R_v} = 0 \quad (9)$$

Equations 4 and 9 are solved simultaneously to obtain σ_1 and σ_2 . A unique solution is obtained in the case of polydisperse constituents because phase composition and phase ratio depend on blend composition. However, if the constituents are monodisperse, phase composition is independent of blend composition, and eqs 4 and 9 are degenerate.

The quantities W_{1i} and W_{2j} were taken from the molecular weight distributions in Figure 1. There were 190 molecular weight fractions provided for each constituent. They were reduced to 19 equal fractions to decrease calculation time. Although phase compositions and number-average chain lengths were not known, they could be written as functions of σ_1 and σ_2 . The Mathematica software was used to solve eqs 4 and 9. Subsequently, eqs 5 and 8 were used to calculate χ and the volume fraction HDPE in the HDPE-poor and HDPE-rich phases, ϕ'_1 and ϕ'_2 , respectively.

Phase Composition and Interaction Parameter. Phase compositions and χ interaction parameters extracted from the polydisperse analysis are collected in Table 3. With increasing temperature, the major phase gradually becomes richer in the minor constituent as it approaches the blend composition. The dependence of

Table 3. HDPE Phase Compositions and χ Interaction Parameter from Polydisperse Analysis

blend constituents	T (°C)	EO/HDPE 70/30			EO/HDPE 60/40			EO/HDPE 40/60			EO/HDPE 30/70			av χ (10 ⁻⁴)
		$\frac{\text{HDPE-poor}}{(\phi_1')}$	$\frac{\text{HDPE-rich}}{(\phi_1'')}$	χ (10 ⁻⁴)	$\frac{\text{HDPE-poor}}{(\phi_1')}$	$\frac{\text{HDPE-rich}}{(\phi_1'')}$	χ (10 ⁻⁴)	$\frac{\text{HDPE-poor}}{(\phi_1')}$	$\frac{\text{HDPE-rich}}{(\phi_1'')}$	χ (10 ⁻⁴)	$\frac{\text{HDPE-poor}}{(\phi_1')}$	$\frac{\text{HDPE-rich}}{(\phi_1'')}$	χ (10 ⁻⁴)	
EO8.5/HDPE62	150	0.22	0.85	11	0.20	0.91	14						12.5 ± 2.1	
	165	miscible			0.38	0.67	8						8.0 ± 0.1	
	180				miscible									
EO8.5/HDPE137	150	0.18	0.81	12	0.11	0.95	20						14.0 ± 5.3	
	165	0.20	0.79	10	0.28	0.75	9						9.5 ± 0.7	
	180	0.26	0.54	8	0.32	0.75	7						7.0 ± 0.7	
	210	miscible			miscible									
EO8.5/HDPE292	210	0.20	0.75	6	0.37	0.55	4						5.0 ± 1.4	
	240	0.27	0.56	4	0.39	0.52	3						3.5 ± 0.7	
	270	miscible			miscible									
EO12.3LMW/HDPE62	150													
	180	0.20	0.71	17									27.0 ± 0.1	
	210	0.25	0.64	14	0.36	0.58	12						17.0 ± 0.1	
	240	0.29	0.56	11	0.39	0.55	11						13.3 ± 1.0	
EO12.3HMW/HDPE62	180				0.23	0.80	16						11.0 ± 0.1	
	210	0.16	0.85	18	0.25	0.79	15						16.0 ± 0.1	
	240	0.21	0.78	15	0.30	0.73	13						16.5 ± 2.1	
	270	0.25	0.73	10									14.0 ± 1.4	
													10.0 ± 0.1	

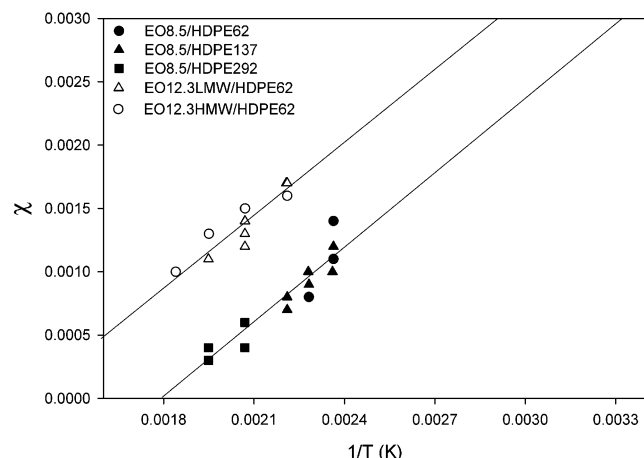


Figure 3. Temperature dependence of the χ interaction parameter.

phase composition on blend composition was previously demonstrated with constituents having relatively narrow molecular weight distributions.²¹ If the molecular weight distribution of one constituent is broad, as is often the case with real polymers exemplified here by HDPE, the phase composition can change dramatically depending on blend composition. For example, as the composition changes from 70/30 to 30/70 (EO/HDPE) and the volume fraction EO-rich phase decreases, the EO-rich phase becomes much richer in HDPE, as seen with ϕ_1' increasing from 0.18 to 0.37 in EO8.5/HDPE137 at 150 °C and from 0.25 to 0.41 in EO12.3LMW/HDPE62 at 210 °C. This reflects the high solubility of low molecular weight HDPE fractions in EO. On the other hand, the solubility of EO in HDPE exhibits much smaller changes with blend composition. The corresponding compositions ϕ_1'' of the HDPE-rich phase are 0.81 and 0.81 in EO8.5/HDPE137 at 150 °C and 0.64 and 0.70 in EO12.3LMW/HDPE62 at 210 °C.

As a general consequence of the high molecular weight tail in the HDPE distribution, an HDPE-rich phase persists in blends with EO as the major constituent at temperatures where blends with HDPE as the major constituent form a single phase. Thus, the 70/30 and 60/40 blends of EO8.5/HDPE137 form two phases at 180 °C, whereas the 40/60 and 30/70 blends are miscible at 180 °C. This can occur even if the constituents are similar in terms of weight-average molecular weight. In EO12.3LMW/HDPE62 blends, compositions that have EO as the major constituent form two phases at 240 °C whereas compositions with HDPE as the major constituent are miscible at this temperature.

The results in Table 3 are consistent with χ independent of blend composition. Although the values of χ scatter, they do not exhibit a systematic change with blend composition. As expected, χ decreases with increasing temperature and decreasing EO octene content, and the blend becomes more miscible. The normal temperature dependence of χ suggests that it follows the relationship²⁹

$$\chi = a + \frac{b}{T} \quad (10)$$

Results for blends of all compositions and with all molecular weights define two linear relationships based on comonomer content, Figure 3. Linear regression gives $a = -0.004$ and $b = 2.0$ with $r^2 = 0.84$ for EO8.5 and $a = -0.003$ and $b = 1.9$ with $r^2 = 0.87$ for EO12.3.

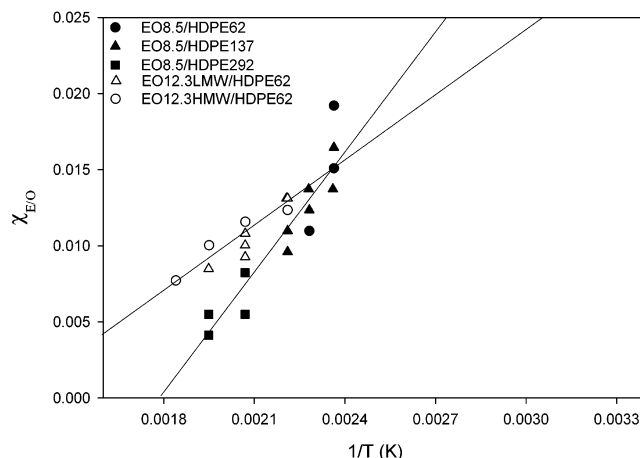


Figure 4. Temperature dependence of the reduced interaction parameter, $\chi_{E/O} = \chi(\psi_2)^{-2}$.

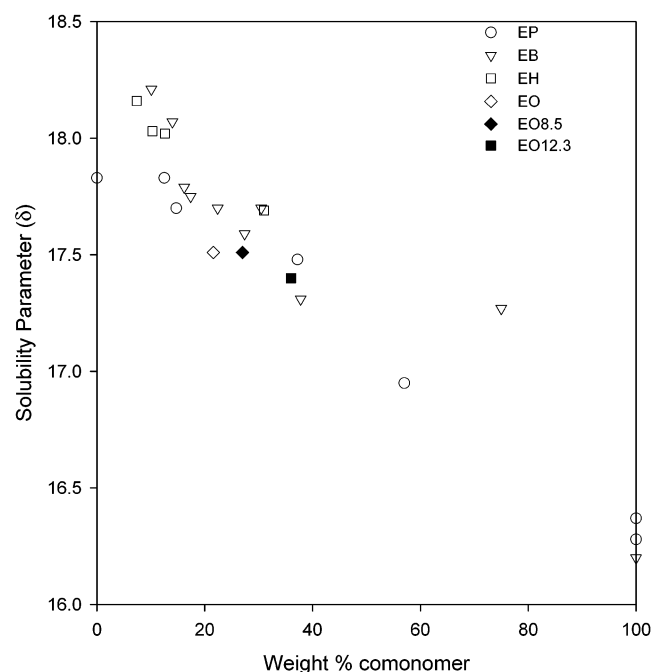


Figure 5. Solubility parameter of EO8.5 and EO12.3 at 166 °C compared with data for ethylene/propylene (EP), ethylene/butene (EB), ethylene/hexane (EH) and ethylene/octene (EO) copolymers from ref 33.

According to the random copolymer theory,^{30,31} blends of statistical copolymers should exhibit a composition dependence of χ according to

$$\chi = \chi_{E/O}(\Delta\psi)^2 \quad (11)$$

where $\chi_{E/O}$ is the segmental interaction parameter of ethylene and octene, and $\Delta\psi = \psi_1 - \psi_2$ with ψ_1 and ψ_2 being the volume fractions of octene in the copolymers. Blends of polydisperse ethylene–styrene copolymers of different styrene content conform to eq 11.²¹ In contrast, blends of model polyolefins obtained by hydrogenation of almost monodisperse polydienes exhibit a systematic increase in the quantity $\chi(\Delta\psi)^{-2}$ with increasing $\Delta\psi$.^{12,32} For EO/HDPE blends $\psi_1 = 0$ and eq 11 reduces to $\chi_{E/O} = \chi(\psi_2)^{-2}$ where ψ_2 is the volume fraction octene in the copolymer. The copolymer equation is tested by plotting the temperature dependence of $\chi(\psi_2)^{-2}$ in Figure 4. The data do not collapse to a single curve, nor do they even

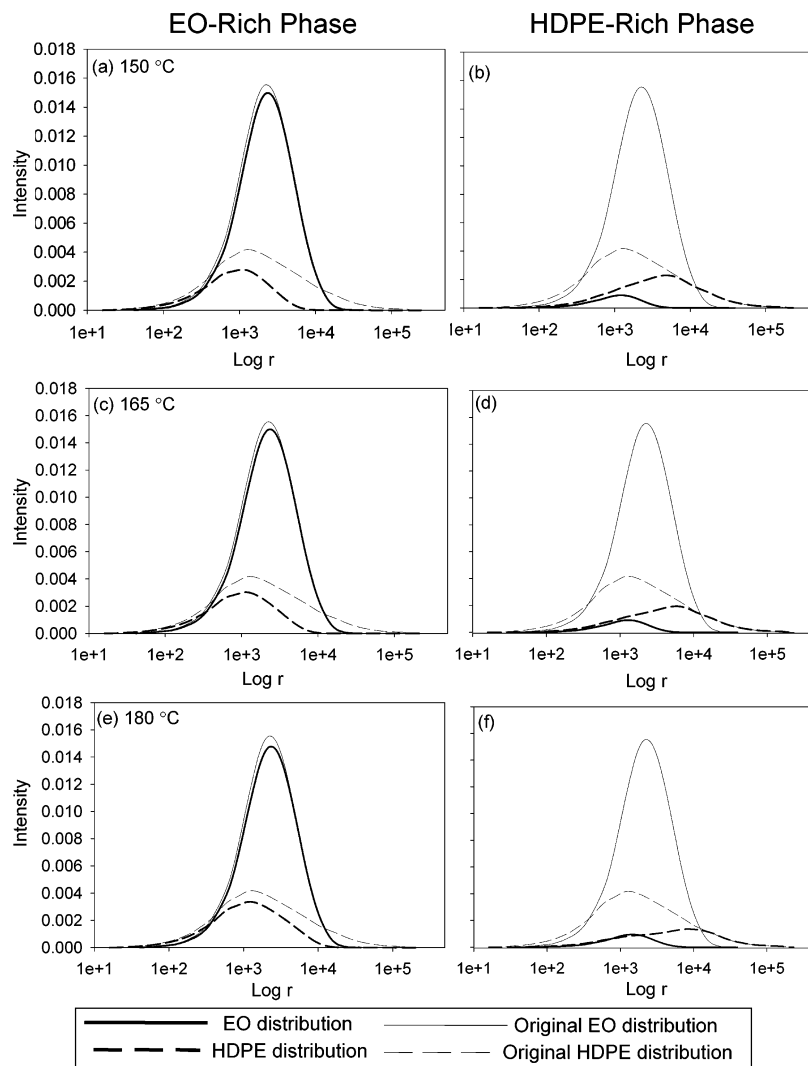


Figure 6. Effect of temperature on calculated molecular weight distributions of EO8.5 and HDPE137 in both phases for blend composition 70/30 (v/v) EO8.5/HDPE137: (a, b) at 150 °C; (c, d) at 165 °C; (e, f) at 180 °C.

exhibit a common temperature dependence. Instead, $\chi_{E/O}$ increases with $\Delta\psi$ as is reported for model polyolefins.

For many polymer blends, χ can be expressed in terms of the solubility parameter difference of the two constituents

$$\chi = \frac{V_{ref}}{RT}(\delta_1 - \delta_2)^2 \quad (12)$$

where δ_1 and δ_2 are solubility parameters of the constituent polymers and V_{ref} is the reference volume. The validity of eq 12 for polyolefin blends has been demonstrated in terms of the relationship between χ and the difference $\delta_1 - \delta_2$ from small-angle neutron scattering (SANS) studies primarily of model polyolefins.¹² The few solubility parameters reported in the literature for real ethylene copolymers include some results from PVT measurements at 166 °C for homogeneous copolymers of ethylene with α -olefins.³³

For purposes of comparison, eq 10 was used to obtain χ values of EO/HDPE blends at 166 °C and the solubility parameter for EO was calculated according to eq 12 using the reported value of $\delta_1 = 17.83 \text{ MPa}^{1/2}$ for a Ziegler–Natta catalyzed HDPE,³³ and $V_{ref} = 35 \text{ cm}^3 \text{ mol}^{-1}$. From χ values of 9.7×10^{-4} and 1.8×10^{-3} for

EO8.5 and EO12.3, respectively, solubility parameters of $17.51 \text{ MPa}^{1/2}$ for EO8.5 and $17.40 \text{ MPa}^{1/2}$ for EO12.3 at 166 °C were obtained. These are plotted in Figure 5 together with results for homogeneous ethylene copolymers obtained from PVT measurements, which were carried out in the melt. Good correspondence provides validation of the polydisperse analysis, which relies on quenching to preserve the phase condition in the melt.

Molecular Weight Distribution. In blends of polydisperse polymers, low molecular weight fractions of one constituent are always more miscible with the other constituent than the high molecular weight fractions. Under conditions where the polydisperse constituents exhibit partial miscibility, both equilibrium phases consist of high molecular weight fractions of the major constituent and low molecular weight fractions of the minor constituent. In other words, the molecular weight distribution of a constituent is not the same in both phases and is not the same as the original distribution. Moreover, the molecular weight distribution in each phase should change with blend composition. As a consequence, phase composition depends on blend composition.

For the HDPEs in this study, increasing molecular weight broadens the overall molecular weight distribution and increases the amount of very high molecular

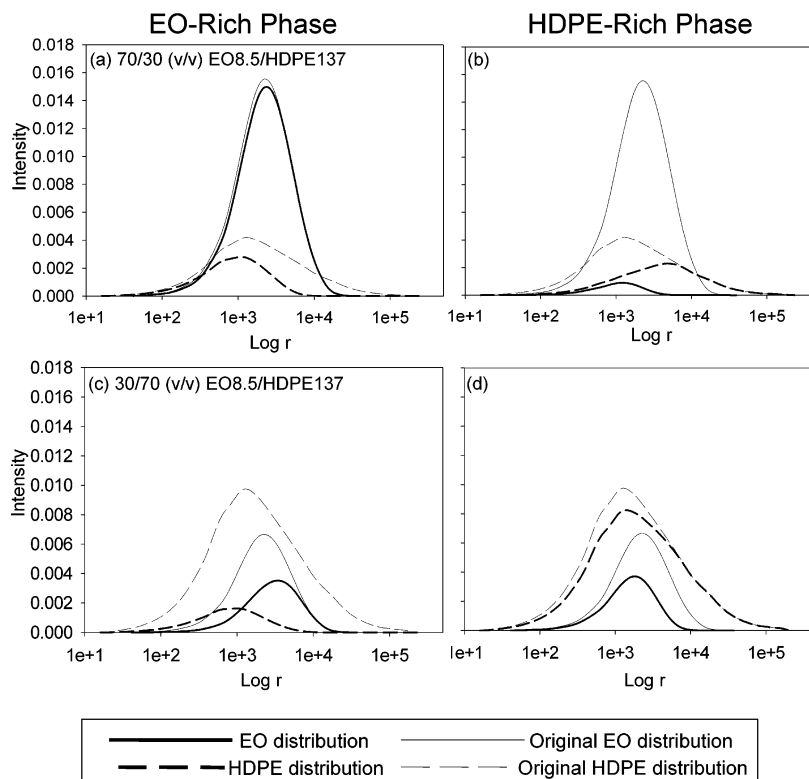


Figure 7. Effect of blend composition on calculated molecular weight distributions of EO8.5 and HDPE137 in both phases at 150 °C: (a, b) 70/30 (v/v) EO8.5/HDPE137; (c, d) 30/70 (v/v) EO8.5/HDPE137.

weight fractions (Figure 1b). The consequences of polydispersity are demonstrated by calculating the molecular weight distribution of each constituent in each phase. The phase compositions ϕ'_{1i} and ϕ''_{1i} for a given fraction with r_{1i} , and likewise ϕ'_{2j} and ϕ''_{2j} for r_{2j} , were calculated from eqs 3 and 7. The calculation was performed for each of the 190 molecular weight fractions provided. Figure 6 shows the effect of increasing temperature on the distributions of EO8.5 and HDPE137 in 70/30 (v/v) blends. The original distribution of each constituent normalized to the blend composition is presented as the thin lines. The constituent distribution in each phase, given as thick lines, is normalized to the phase composition. In terms of phase composition, the gradually increasing concentration of the minor constituent with increasing temperature is evident in both the EO-rich phase and the HDPE-rich phase. Molecular weight fractionation in the 70/30 blends is much more evident with the broad disperse HDPE than with the relatively narrow disperse EO. Comparison of the molecular weight distribution of HDPE in the constituent-poor and constituent-rich phases demonstrates the preferential dissolution of lower molecular weight HDPE fractions in the EO-rich phase. As the temperature increases from 150 to 180 °C, the distribution of HDPE in the EO-rich phase broadens to include higher molecular weight fractions, nevertheless leaving the high molecular weight tail in the HDPE-rich phase.

The minor constituent of the blend most readily demonstrates molecular weight fractionation because it is more or less equally distributed between the two phases. To illustrate fractionation of EO, constituent molecular weight distributions in both phases of the EO8.5/HDPE137 70/30 blend at 150 °C are shown again in Figure 7 compared with the distributions in the 30/70 blend at the same temperature. Preferential solution of lower molecular weight fractions of EO in HDPE is

immediately apparent in the 30/70 blend even though this polymer is considered to have relatively narrow molecular weight distribution.

Summary

An approach previously used to characterize phase behavior in blends of chemically similar amorphous copolymers was successfully extended to blends of crystallizable polyolefins. Although chemical similarity of the constituents precluded conventional methods for imaging domain morphology of polyolefin blends, the modulus difference between the phases was large enough that the domain morphology could be probed using AFM. Homogeneous ethylene–octene copolymers with 5.3 mol % comonomer were completely miscible with high-density polyethylene, whereas copolymers with 8.3 and 12.3 mol % comonomer provided a composition window of partial miscibility that revealed the effects of temperature and constituent molecular weight. The study confirmed the UCST behavior of blends comprised of high density polyethylene and a homogeneous ethylene–octene copolymer. This study also considered the effect of molecular weight distribution in real polyolefins on the phase behavior in blends. In particular, it demonstrated the general consequences for phase behavior of the low and high molecular weight tails on the broad distribution of HDPE. The low molecular weight tail readily dissolved in EO to highly enrich the EO-rich phase especially when EO was the minor constituent. Conversely, when HDPE was the minor constituent low solubility of high molecular weight HDPE fractions led to persistence of a HDPE-rich phase to higher temperatures. Even in EO copolymers with relatively narrow molecular weight distribution, fractionation of low molecular weight fractions into the HDPE-rich phase was clearly evident.

Acknowledgment. The authors thank Dr. Hongyu Chen and Dr. Wilson Cheung for many helpful discussions. The financial support of BP Chemicals is gratefully acknowledged.

References and Notes

- (1) Defoor, F.; Groeninckx, G.; Reynaers, H.; Schouterden, P.; Van der Heijden, B. *Macromolecules* **1993**, *26*, 2575–2582.
- (2) Defoor, F.; Groeninckx, G.; Reynaers, H.; Schouterden, P.; Van der Heijden, B. *J. Appl. Polym. Sci.* **1993**, *47*, 1839–1848.
- (3) Mirabella, Jr., F. M.; Westphal, S. P.; Fernando, P. L.; Ford, E. A.; Williams, J. G. *J. Polym. Sci., Part B: Polym. Phys.* **1988**, *26*, 1995–2005.
- (4) Wignall, G. D.; Alamo, R. G.; Londono, J. D.; Mandelkern, L.; Stehling, F. C. *Macromolecules* **1996**, *29*, 5332–5335.
- (5) Alamo, R. G.; Graessley, W. W.; Krishnamoorti, R.; Lohse, D. J.; Londono, J. D.; Mandelkern, L.; Stehling, F. C.; Wignall, G. D. *Macromolecules* **1997**, *30*, 561–566.
- (6) Agamalian, M.; Alamo, R. G.; Kim, M. H.; Londono, J. D.; Mandelkern, L.; Wignall, G. D. *Macromolecules* **1999**, *32*, 3093–3096.
- (7) Choi, P. *Polymer* **2000**, *41*, 8741–8747.
- (8) Bates, F. S.; Wignall, G. D.; Koehler, W. C. *Phys. Rev. Lett.* **1985**, *55*, 2425–2428.
- (9) Graessley, W. W.; Krishnamoorti, R.; Balsara, N. P.; Fetters, L. J.; Lohse, D. J.; Schulz, D. N.; Sissano, J. A. *Macromolecules* **1993**, *26*, 1137–1143.
- (10) Alamo, R. G.; Londono, J. D.; Mandelkern, L.; Stehling, F. C.; Wignall, G. D. *Macromolecules* **1994**, *27*, 411–417.
- (11) Agamalian, M. M.; Alamo, R. G.; Londono, J. D.; Mandelkern, L.; Wignall, G. D. *J. Appl. Crystallogr.* **2000**, *33*, 843–846.
- (12) Lohse, D. J.; Graessley, W. W. In *Polymer Blends*; Paul, D. R., Bucknall, C. B., Eds.; Wiley-Interscience: New York, 2000; Vol. 1, Formulation, p 219.
- (13) Reichart, G. C.; Graessley, W. W.; Register, R. A.; Lohse, D. J. *Macromolecules* **1998**, *31*, 7886–7894.
- (14) Wignall, G. D.; Londono, J. D.; Lin, J. S.; Alamo, R. G.; Galante, M. J.; Mandelkern, L. *Macromolecules* **1995**, *28*, 3156–3167.
- (15) Hill, M. J.; Morgan, R. L.; Barham, P. J. *J. Macromol. Sci.—Phys.* **1999**, *B38*, 37–50.
- (16) Crist, B.; Hill, M. J. *J. Polym. Sci., Part B: Polym. Phys.* **1997**, *35*, 2329–2353.
- (17) Hill, M. J.; Barham, P. J. *Polymer* **1997**, *38*, 5595–5601.
- (18) Bensason, S.; Nazarenko, S.; Chum, S.; Hiltner, A.; Baer, E. *Polymer* **1997**, *38*, 3513–3520.
- (19) Tanem, B. S.; Stori, A. *Polymer* **2001**, *42*, 4309–4319.
- (20) Chen, H. Y.; Cheung, Y. W.; Hiltner, A.; Baer, E. *Polymer* **2001**, *42*, 7819–7830.
- (21) Chen, H. Y.; Chum, S. P.; Hiltner, A.; Baer, E. *Macromolecules* **2001**, *34*, 4033–4042.
- (22) Bensason, S.; Minick, J.; Moet, A.; Chum, S.; Hiltner, A.; Baer, E. *J. Polym. Sci., Part B: Polym. Phys.* **1996**, *34*, 1301–1315.
- (23) Van Krevelyn, D. W. *Properties of Polymers*, 3rd ed.; Elsevier: Amsterdam, 1990; p 120.
- (24) Olley, R. H.; Bassett, D. C. *Polymer* **1982**, *23*, 1707–1710.
- (25) Flory, P. J. *Principles of Polymer Chemistry*; Cornell University Press: Ithaca, NY, 1953; Chapter 12.
- (26) Vanhee, S.; Koningsveld, R.; Berghmans, H.; Solc, K.; Stockmayer, W. H. *Macromolecules* **2000**, *33*, 3924–3931.
- (27) Solc, K.; Koningsveld, R. *Collect. Czech. Chem. Commun.* **1995**, *60*, 1689–1718.
- (28) Koningsveld, R.; Solc, K. *Collect. Czech. Chem. Commun.* **1993**, *58*, 2305–2320.
- (29) Utracki, L. A. *Polymer Alloys and Blends*; Hanser: Munich, Germany, 1989; Chapter 2.
- (30) Scott, P. J. *J. Polym. Sci.* **1952**, *9*, 423–432.
- (31) ten Brinke, G.; Karasz, F. E.; MacKnight, W. J. *Macromolecules* **1983**, *16*, 1827–1832.
- (32) Graessley, W. W.; Krishnamoorti, R.; Balsara, N. P.; Butera, R. J.; Fetters, L. J.; Lohse, D. J.; Schulz, D. N.; Sissano, J. A. *Macromolecules* **1994**, *27*, 3896–3901.
- (33) Han, S. J.; Lohse, D. J.; Condo, P. D.; Sperling, L. H. *J. Polym. Sci., Part B: Polym. Phys.* **1999**, *37*, 2835–2844.

MA021621A